

# Variational Quantum Eigensolver: A Comparative Analysis of Classical and Quantum Optimization Methods

Duc-Truyen Le\*

*Department of Physics,*

*National Tsing Hua University,  
Hsinchu, Taiwan 300044, R.O.C.*

Vu-Linh Nguyen

*Department of Theoretical Physics, University of Science,  
Vietnam National University, Ho Chi Minh City 70000, Vietnam*

Ha C. Nguyen

*Département de Physique de l'École normale supérieure,  
Université PSL, 75005 Paris, France*

Hung Q. Nguyen

*Nano and Energy Center, University of Science,  
Vietnam National University, Hanoi, Vietnam*

Van-Duy Nguyen†

*Phenikaa Institute for Advanced Study,  
Phenikaa University, Hanoi 12116, Vietnam*  
(Dated: April 21, 2025)

**Abstract:** In this study, we study the Variational Quantum Eigensolver (VQE) application for the Ising model as a test bed model, in which we pivotally delved into several optimization methods, both classical and quantum, and analyzed the quantum advantage that each of these methods offered, and then we proposed a new combinatorial optimization scheme, deemed as QN-SPSA+PSR which combines calculating approximately Fubini-study metric (QN-SPSA) and the exact evaluation of gradient by Parameter-Shift Rule (PSR). The QN-SPSA+PSR method integrates the QN-SPSA computational efficiency with the precise gradient computation of the PSR, improving both stability and convergence speed while maintaining low computational consumption. Our results provide a new potential quantum supremacy in the VQAs's optimization subroutine, even in Quantum Machine Learning's optimization section, and enhance viable paths toward efficient quantum simulations on Noisy Intermediate-Scale Quantum Computing (NISQ) devices. Additionally, we also conducted a detailed study of quantum circuit ansatz structures in order to find the one that would work best with the Ising model and NISQ, in which we utilized the properties of the investigated model.

**Keyword:** Ising Model, Variational Quantum Algorithm, Quantum Optimization, Ansatz Construction, Gradient Estimation

## I. INTRODUCTION

From the early stage of studying quantum computers, that by its very quantum nature is promising for a bright new age of computation coming along with three crucial keys of quantum theory: quantum probabilistics, superposition, and entanglement. The distinct properties of quantum computers (QC) from classical computers make it be more unique in application, not only be an upgraded computational speed version of traditional computers. Currently, when the quantum hardware is rather limited on operational stats and noise resilience, despite of the ambiguity of the realization of such advantages, Variational Quantum Algorithms (VQAs) [1, 2] are thought to be the best at outperforming conventional computers,

which are able to implement well on near-term quantum devices known as the so-called Noisy Intermediate-Scale Quantum (NISQ) computers [3–7].

Nowadays, when the quantum revolution is being on track, big tech companies like IBM, Google, D-Wave, etc. compete to build their own quantum computers to yield quantum supremacy, where the first-ever experimental demonstration was achieved by the Google AI Quantum team [8], but that is still far from what we expect the quantum computer could do, while coherence time, connectivity of qubits, and qubit number limitations keep us from being able to successfully run a long-depth circuit and produce a significant result on the present noisy device, in addition to quantum gate implementation issues. Those restrictions would yet be challenging to hardware scientists in the near future, posing obstacles that computer scientists would need to weigh against trainability, precision, and efficiency, nevertheless, these NISQ devices are capable of exploitation, see Ref. [9] for fur-

\* leductruyenphys@gapp.nthu.edu.tw

† duy.nguyenvan@phenikaa-uni.edu.vn

ther reviews. Standing out among quantum algorithms envisioned to beat classical computers, which are mostly designed for the fault-tolerant quantum computer, VQAs turn up regarded as an appropriate candidate compatible with the current defective quantum device to address these constraints [2]. The first two prominent applications of VQAs coming up are the Variational Quantum Eigensolver (VQE) [10] and the Quantum Approximate Optimization Algorithm (QAOA) [11]. These inherit the core scheme of a VQA, which is to utilize the hybrid routine, leverage the versatility and computational power of classical computers to handle the computation processing, and use quantum devices to execute the quantum circuit. Hence, in this paper's scope, we will travel through the standard procedures of VQE and investigate the properties of different optimization methods implemented in the VQE's subroutine.

The structure of this paper is as follows: in Chapter 2, we provide an overview of the Variational Quantum Eigensolver (VQE) procedures, a brief introduction to the Transverse Ising Model, and its symmetries are also discussed here, which will be utilized to inform the ansatz structure. Subsequently, Chapter 3 delves into optimization methods, encompassing both classical and quantum approaches, where we will propose a new quantum optimization method. The numerical study and experiment are conducted in Chapter 4, and then we make the final conclusion in Chapter 5.

## II. VARIATIONAL QUANTUM EIGEN SOLVER FOR ISING MODEL

### A. Overview

VQE was initially proposed by Peruzzo et al. [10, 12] as an efficient alternative way to compute the ground state energy, or expanded to estimate the higher-energy levels [13–17], of many quantum chemistry systems [18, 19] or many-body systems, i.e.  $H_2$  [20, 21], LiH and  $BeH_2$  [22] molecules, rather than Quantum Phase Estimation (QPE) [23] which demands impractically huge numbers of quantum gates. Besides that, applications of VQE in drug discovery [24, 25] and materials [26–28] are considerably concerned. Consequently, VQE becomes a highly flexible, viable strategy with current potential quantum resources that can outpace conventional computers [29, 30]. Following the success of running on the photonic quantum processor combined with the traditional devices, many research works favor the development of various types of VQA reviewed in Ref. [9, 31]. In essence, what makes VQE (generally VQAs) engrossing is the trial state analysis step to choosing an ansatz adaptive to particular quantum device architecture and/or problems. Subsequently, the suitable ansatz is executed congruently on the NISQ device, the remainders are then handled by the classical computer with the hybrid loop to generate remarkable results with the aid of error mitigation tech-

niques. Instead of diagonalizing a matrix representation of Hamiltonian  $\hat{H}$  to find out eigenvalues that exponentially scale up the matrix size and calculation overhead in traditional computing as the problem grows up larger, VQE just focuses on catching up with the ground state energy  $E_g$ , basically based on the variational principle

$$E_g \leq E[\Psi(\boldsymbol{\theta})] = \frac{\langle \Psi(\boldsymbol{\theta}) | \hat{H} | \Psi(\boldsymbol{\theta}) \rangle}{\langle \Psi(\boldsymbol{\theta}) | \Psi(\boldsymbol{\theta}) \rangle} = \langle \hat{H} \rangle_{\hat{U}(\boldsymbol{\theta})}. \quad (1)$$

The arbitrary quantum state  $|\Psi(\boldsymbol{\theta})\rangle \equiv \hat{U}(\boldsymbol{\theta})|\Psi_0\rangle$  is a trial solution, the so-called *ansatz* parametrized by a unitary operator  $\hat{U}(\boldsymbol{\theta})$ , so that when the parameter  $\boldsymbol{\theta}$  varies, the ansatz  $|\Psi(\boldsymbol{\theta})\rangle$  is readily capable of spanning on the relevant quantum space where the ground state is located. By modifying  $\boldsymbol{\theta}$  value systematically, the VQE task is to travel around spanned space to extract the ground state minimizing the energy function  $E[\Psi(\boldsymbol{\theta})]$  or, in general VQA, the energy function described by  $\mathcal{L}(\boldsymbol{\theta}, \langle \hat{H} \rangle_{\hat{U}(\boldsymbol{\theta})})$ , and the objective is

$$\min_{\boldsymbol{\theta}} \mathcal{L}(\boldsymbol{\theta}, \langle \hat{H} \rangle_{\hat{U}(\boldsymbol{\theta})}). \quad (2)$$

In fact, the optimal wave function is not necessarily required to be close to the ground state solution, due to the error in energy being in the second order of the quantum state error. Formally, the classical approach for VQE insists on an analytical expression of the loss function  $\mathcal{L}(\boldsymbol{\theta}, \langle \hat{H} \rangle_{\hat{U}(\boldsymbol{\theta})})$ , in particular, the wave function expression  $|\Psi(\boldsymbol{\theta})\rangle$  that eventually becomes unachievable going along with more and more problem complexities. Nevertheless, this weakness is literally the quantum advantage we have in the VQE quantum computing approach. Quantum computers are adopted to simulate quantum states, and state expectation outcomes are subsequently measured to pipeline to calculate the loss function classically. And partly because of the loss function precision being greater quadratically than the state function, indeed, we need two states to sandwich operators. VQEs are hereby friendly with noisy devices, which can work out meaningful results even though the states are disturbed by noise. These motivations are robust enough to let us dive deeper into VQE operation, ideally with a noise-free assumption in this paper's scope though, the noisy one will be addressed in a future study.

The structure of a VQE algorithm is depicted schematically as Fig. 1 within four basic steps: *Hamiltonian construction*, *Ansatz preparation*, *measurement strategy*, and *Optimization*.

*Hamiltonian construction:* Starting from a given abstract problem, e.g., molecule ground state energy, shortest path, transshipment problems, an initially mathematical form called the Hamiltonian  $\hat{H}$  is modeled. A mapping scheme is needed to convert  $\hat{H}$  into a new form made out of operators that are able to execute on a quantum computer. Invoking prior knowledge of the physical system, particular symmetries are drawn on to simplify the

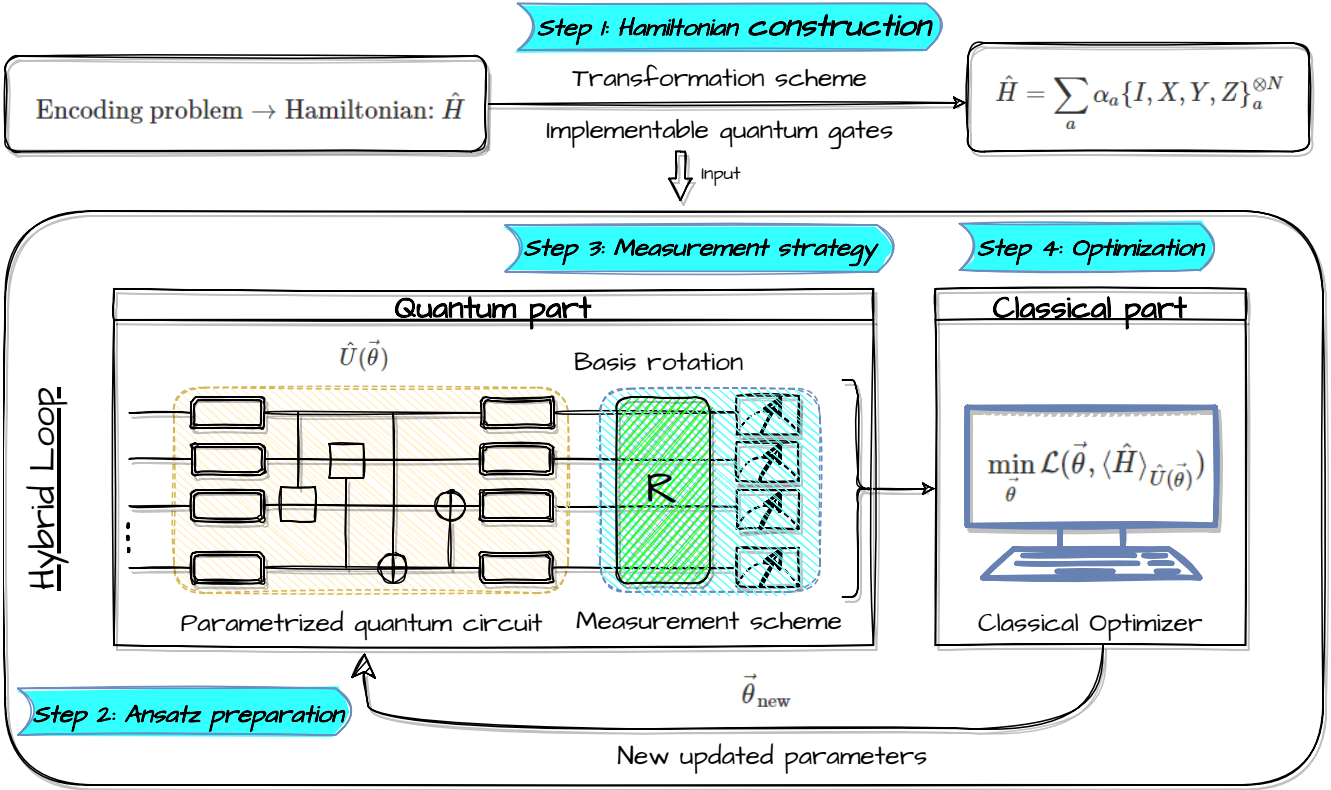


FIG. 1: Variational Quantum Eigensolver (VQE) Architecture. This schematic representation illustrates the workflow of the VQE algorithm, which is a hybrid quantum-classical optimization technique used to estimate the ground state energy of a given Hamiltonian. The process consists of four key steps: Hamiltonian Construction (Step 1): The problem is encoded into a Hamiltonian  $\hat{H}$ , expressed as a weighted sum of Pauli operator products acting on  $N$  qubits; Ansatz Preparation (Step 2): A parametrized quantum circuit is constructed by unitary operator  $\hat{U}(\theta)$ , where  $\theta$  represents tunable parameters; Measurement Strategy (Step 3): The expectation value  $\langle \hat{H} \rangle$  is obtained by applying a basis rotation followed by a specific measurement scheme; Optimization (Step 4): The measured expectation value is fed into a classical optimizer, which minimizes energy  $\langle \hat{H} \rangle_{\hat{U}(\theta)}$  by updating the parameters  $\theta$ , this step is the crucial point that we will dig into details within this study. The Hybrid Loop, where quantum computations (state preparation and measurement) are performed on a quantum processor, while classical optimization is handled by a classical computer. The updated parameters  $\theta_{\text{new}}$  are fed back into the quantum circuit iteratively.

Hamiltonian, such information is usefully reused to guide the erection of other VQE subroutines.

*Ansatz preparation:* To pick out a good ansatz, an essential condition that must be satisfied is that the space spanned by the ansatz contains the desired state to extremize the objective function, more details can be found in Ref. [32]. An obvious one is a generic ansatz spread over all Hilbert space, a quantum circuit for that kind of ansatz is usually generated by multi-control- $U_3(\theta)$  gates so that all problems could be ultimately settled without ansatz concern. Nevertheless, that is not the end of the story, the computation cost of such a multi-control- $U_3(\theta)$  gate is extremely high and even unfeasible when deployed on the NISQ device. As a consequence, an initial crucial step in VQE is to find an ansatz that is expressive enough to capture the important features of the

wavefunction but also efficient enough to be optimized using optimization techniques. In this article, we employ the approach that excavates up symmetries and physical properties of the physical system to guide the design of the ansatz respecting those symmetries, which helps us considerably reduce the number of training parameters and circuit depth needed in a theoretically speculative way, thereby improving the efficiency of the optimization. There are also other methods that use a hierarchical ansatz, where the circuit is divided into layers and each layer is optimized independently, and also use machine learning to automatically generate the quantum circuit [33, 34].

*Measurement:* To read off information from the wave function to estimate the expectation value of the Hamiltonian, apart from the standard basis measurement

where each qubit in the output state is measured in the computational basis, the measurement scheme is manifestly came up with is a unitary transformation to the diagonal basis of observable operators in the Hamiltonian, typically defined by tensor products of Pauli operators, such as X, Y, and Z. Almost all Hamiltonians of interest are Hermitian and able to decompose in terms of Pauli strings.

$$\hat{H} = \sum_i \otimes_{j=1}^N \sigma_j^i, \quad (3)$$

$$\sigma_j^i \in \{I, X, Y, Z\},$$

each Pauli string term  $P^i = \otimes_{j=1}^N \sigma_j^i$  has likely overlapped the others in somewhere qubit sites, which means  $\sigma_j^m \equiv \sigma_j^k$  can be measured simultaneously. The grouping methods skillfully make use of this information to lower the number of measurements, the symmetry structures of the problem are able to exploit as well, and other efficient measurement methods are reviewed in [35]. Those on-research topics are highly crucial to the current NISQ device when a minimum measurement performance is required upon a given restricted number of shots. Furthermore, for a given  $\epsilon$  accuracy, VQE demands a trade-off between the  $\mathcal{O}(\frac{1}{\epsilon^2})$  number of circuit samples and  $\mathcal{O}(1)$  circuit depth with other finding ground state energy methods such as QPE, which consumes  $\mathcal{O}(1)$  circuit measurement repetitions with depth  $\mathcal{O}(\frac{1}{\epsilon})$ . A better approach is essentially proposed to reconcile disadvantages between the two above methods, which is deemed a generalized VQE algorithm,  $\alpha$ -VQE, when outrunning VQE by just  $\mathcal{O}(\frac{1}{\epsilon^{2(1-\alpha)}})$  circuit samples and lower circuit depth  $\mathcal{O}(\frac{1}{\epsilon^\alpha})$  than QPE, where  $\alpha \in [0, 1]$  [36].

*Optimization:* Last but not least, the last piece in the VQE subroutine is to vary the parameter  $\theta$  to catch up with the global extreme point (but in many cases, the local one is preferred) in the function of interest described by Eq. (2). The criteria should be pondered for problem-friendly implementation, which are able to perform low-cost function evaluation, fast convergence with a given quantum of resources, and silence to noise. Based on different kinds of utilizing objective function information, people classify it into two main optimization approaches: gradient-based and derivative-free. Meanwhile, the gradient-based approach employs the gradient information in mostly first order, and second order to travel along the steepest direction of the cost function landscape. The derivative-free rather directly uses responses of the objective function at different points in the parameter space to iteratively improve the parameter values, and as usual, these utilize the classical algorithm subroutine and just consume a limited quantum evaluation expense compared to gradient-based, these are thus seemingly more congruous with NISQ. In the context of VQAs, gradient-free approaches can be used to optimize quantum circuit parameters when computing the gradient is either impractical or excessively costly, for example, when simulating the behavior of a quantum system becomes computationally expensive, or when the objec-

tive function cannot be expressed analytically. Nevertheless, the gradient-based methods are arguably more reliable and have faster convergence as the more complicated structure of the objective function, henceforth, the total trade-off would be shoulder-by-shoulder when deliberately adopting between these two. Furthermore, the step size problem in gradient-based and applying machine learning in derivative-free are active topics of research at this stage, see [9] section II.D for more reviews. In the context of this paper, we investigated several optimization methods and instead labeled them again into two regimes: classical and quantum optimization.

## B. Transverse Ising model

The Transverse Ising model (TIM) was introduced first in 1963 by de Gennes when he built a model for describing the low-frequency collective modes of protons in the ferroelectric phase of ferroelectric crystals  $\text{KH}_2\text{PO}_4$  [37]. From then until now, the Transverse Ising Model has been used to represent enormous simple-to-complex systems such as brain science and information science and technology.

We consider the 1D Transverse Ising ring, describing the nearest-neighbor interactions of the spin projection along the z-axis and uniform external magnetic field along the x-axis (in principle, perpendicular to the z-axis). Defined by the two-spin exchange interaction factor  $J$  and representative strength of the external field  $h$  as described below

$$\hat{H}_{\text{TIM}} = -J \sum_{n=1}^N \sigma_{n-1}^z \sigma_n^z - h \sum_{n=0}^{N-1} \sigma_n^x. \quad (4)$$

The Hamiltonian in Eq. (4) possesses a  $\mathbf{Z}_2$  symmetry remaining invariant under spin-flipping action. When the coupling constant is  $h < 1$ , the system exhibits a ferromagnetic phase, and the spins favorably align along the z-direction. Conversely, for  $h > 1$ , the system transitions to a disordered paramagnetic phase. The  $\sigma_x$  terms take a dominant role when  $h \rightarrow \infty$ , leading the ground state to align predominantly in the  $|+\rangle^{\otimes N}$  state. At the critical point,  $h = 1$  renders the gapless property in the thermodynamic limit.

One of the key differences between the classical and quantum versions of the Ising model is that the expectation value of two terms in Eq. (4) must be measured separately due to the non-commutative feature of these elements. However, the commutation property allows us to perform only two observations to extract the Hamiltonian's expectation. The first term  $\sum_{n=1}^{N-1} \sigma_{n-1}^z \sigma_n^z$  can be cumulatively achieved by measuring directly on the computational basis as follows:

$$\langle \sigma_m^z \sigma_n^z \rangle = \sum_{\{q_0, \dots, q_{N-1}\} = \{0,1\}} |a_{q_0 \dots q_m \dots q_n \dots q_{N-1}}|^2 (-1)^{q_m + q_n}, \quad (5)$$

$$\langle \sigma_n^z \rangle = \sum_{\{q_0, \dots, q_{N-1}\} = \{0,1\}} |a_{q_0 \dots q_n \dots q_{N-1}}|^2 (-1)^{q_n}, \quad (6)$$

with  $|a_{q_0 \dots q_m \dots q_n \dots q_{N-1}}|^2$  and  $|a_{q_0 \dots q_n \dots q_{N-1}}|^2$  are the probabilities of being in the computational basis state  $|q_0 \dots q_m \dots q_n \dots q_{N-1}\rangle$  and  $|q_0 \dots q_n \dots q_{N-1}\rangle$  respectively. Similarly,  $\sum_{n=0}^{N-1} \sigma_n^x$  is obtained by applying the Hadamard gate or the  $R_y\left(-\frac{\pi}{2}\right)$  gate in advance to transform to the Z-basis, or computational basis, and then taking the measurements following Eq. (6).

### C. Ansatz Construction

To construct an ansatz in terms of a parameterized quantum circuit (PQC), as mentioned above, we need the  $U(\theta)$  operator to be able to span all quantum Hilbert space so that we can use it to solve all issues. Indeed, we do not, in practice though, a general  $U(\theta)$  operator that is hard to implement experimentally because of the noisy and weighty composite  $C - U_3$  gate and actually does not acquire overall good operation even in an ideal simulator. Hence, the ansatz implementation for a particular problem's purpose is a serious studying process of the VQE working roadmap. In addition to the compatibility with the current quantum device, tapping into symmetries and properties of our problem could be leveraged to shrink the parameter space, which are the important criteria for adopting an ansatz.

#### 1. Symmetry of the Transverse Ising model

At the scope of this article, we consider three properties of TIM so that we take its suggesting information into account to decrease the size of the ansatz

- *Real representation.* Using the eigenstates of the  $\sigma_z$  (Pauli-z) operator as the elementary binary computational basis, in terms of which,  $\sigma^z$ ,  $\sigma^x$  are real matrices, due to that, we can represent the TIM Hamiltonian in real form, the eigenstates of the TIM Hamiltonian can thus be chosen to be real for conventional purposes. Namely, considering  $|\Psi\rangle = \sum_n C_n |n\rangle$  is an eigenstate of  $H_{\text{TIM}}$  expanding in the computational basis  $|n\rangle$ . The real form of  $H_{\text{TIM}}$  means the Hermitian real element matrix that induces coefficients satisfying  $C_n^* C_m = C_n C_m^*$   $\forall m, n \in [0, 2^N - 1]$ , then, in generality

$$C_n = r_n e^{i(c+k_n\pi)}, \quad c \text{ is a constant}, \quad (7)$$

or, in other words, the angles in the complex plane of coefficients  $C_n$  differ from every other by a factor  $k\pi$ , where  $k$  and  $k_n$  are integers. Then, the complex angle can be shifted to the real coefficient  $C_n^* = C_n$  by according to the quantum global phase principle.

- *Local interaction.* The first term  $\hat{H}_{\text{TIM}}^{\text{LI}}$  in the TIM Hamiltonian describes the kind of neighboring spin interaction along the z-axis

$$\hat{H}_{\text{TIM}}^{\text{LI}} = \sum_{n=1}^{N-1} \sigma_{n-1}^z \sigma_{n+1}^z. \quad (8)$$

The interaction of two local spins formulated by this term causes a sort of entanglement structure between every two local spins of the ground state energy. Nevertheless, in the case of the order phase, when the external magnetic field is dominant, this interaction can be broken down, each spin will be freely interacting and align in the same direction as the magnetic field.

- *Total spin-flip symmetry.* The most featured symmetry of the Ising model can be referred to as the classical counterpart, time-reversal symmetry (generally,  $\mathcal{Z}_2$  symmetry). Under the total spin-flip transformation in the z direction  $(\sigma^x)^{\otimes N}$

$$[(\sigma^x)^{\otimes N}, \hat{H}_{\text{TIM}}] = 0, \quad (9)$$

which implies the TIM Hamiltonian remains unchanged. This one leads to the eigenstate  $|\Psi\rangle$  and  $(\sigma^x)^{\otimes N} |\Psi\rangle = |\tilde{\Psi}\rangle$  has the same energy, the relation between them is thus put in two cases

$$\langle \Psi | \tilde{\Psi} \rangle = \begin{cases} 0 & \text{Degeneracy} \\ \pm 1 & \text{Non-degeneracy} \end{cases}, \quad (10)$$

where, in the degenerate case, it  $g = 0$  is trivial, and in the non-degenerate  $g > 0$  case, the expanded coefficients in the z-direction basis representation have a structure

$$C_n = \pm C_{2^N - 1 - n}. \quad (11)$$

#### 2. Ansatz selection

For the chosen ansatz, the conventional real coefficients of eigenstates tell us that it is enough to span in real quantum parameter space for finding the ground state energy, and the linear entanglement mapping comes from the information of the local interaction term in the Hamiltonian. Moreover, to accommodate the device constraints, in a speculative way, the available common-use RealAmplitudes ansatz is our good candidate for the implementation, which uses only the quantum gate  $R_y(\theta)$  for the parameterized quantum circuit and the entanglement scheme as in Fig. 2a.

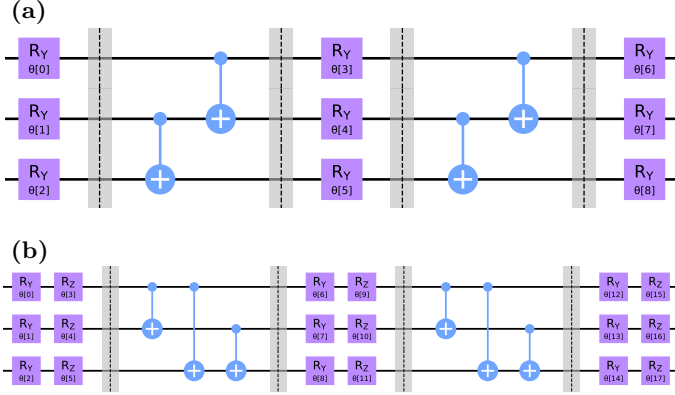


FIG. 2: The two hardware-efficient ansatz investigated in this study: a) RealAmplitudes circuit with the linear entanglement scheme and b) EfficientSU2 circuit with the full entanglement scheme. The rotation gate  $R_Y$  can steer state within real space. Additionally, the single-qubit SU2-group-rotation gates  $\{R_X, R_Y, R_Z\}$  and CNOT gate connecting qubits are practically implemented at scale.

The additional reason for choosing such a Hardware-efficient ansatz architecture [22] comes from the efficient implementation of quantum optimization to attain our full quantum algorithm purpose, which will be addressed in the next subsection III B.

To efficiently travel around the full quantum Hilbert space, we need to tune  $2^{N+1} - 2$  degrees of freedom,  $+1$  inside of the exponent indicates the complex number condition and  $-2$  turns up from normalization and global phase conditions. After bringing TIM's properties, we investigated from section II C 1 to dissect. *Real representation* Eq. (7) helps us eliminate  $+1$  within the exponent, and *Total spin-flip symmetry* Eq. (11) reduces the number of parameters we have to search the ground state by half. Finally,

$$2^{N+1} - 2 \rightarrow 2^{N-1} - 1. \quad (12)$$

The number of layers  $L$ , which changes directly with the ansatz number of parameters  $p$  according to  $p = N(L + 1)$ . Following Eq. (12), we roughly evaluate a necessary number of layer

$$L \geq \frac{2^{N-1} - 1}{N} - 1, \quad (13)$$

notes that this is not a rigorous required condition because the ansatz's entanglement mapping scheme used also contributes, which is able to change the bound as well, it is still a good estimation for surface analysis, nonetheless. Yet, we can realize that, not only TIM, but also Eq. (12) holds for all symmetrically real Hamiltonians being symmetric under  $(\sigma^x)^{\otimes N}$  the operator. Therefore, there are some hidden TIM properties that we are unable to analytically incorporate to give an exact boundary value of  $L$ . Through conducting the experimental survey though, we are able to choose a reliable

value, as we will see in chapter IV B, it works well even for choosing  $L = 2$  for all qubit scaling.

### III. OPTIMIZATION

The next subroutine in the VQE work map, where the optimization of variational parameters plays a key role in hybrid quantum-classical algorithms, and requires efficient methods to achieve fast and accurate convergence. The choice of optimization methods directly impacts the performance of the whole algorithm, influencing their ability to reach optimal solutions with minimal computational cost. Our goal is to investigate different optimization techniques, analyzing their performance to enhance computational efficiency and stability.

Effective optimization methods are essential not only for VQE but also for other variational approaches for quantum chemistry, material simulations and combinatorial optimization tasks. For broader applications, in Quantum Machine Learning (QML) that plays a critical role in training quantum neural networks, kernel-based models, and generative learning algorithms.

In this work, we focus on the Transverse Ising Model as a test bench, where we minimize the cost function defined as the expectation value of the Hamiltonian,  $\langle \hat{H}_{\text{TIM}} \rangle$ , using common methods of optimization categorized into two class operations.

#### A. Classical Operation

Classical operation means regardless of the analysis of the quantum structure of the cost function, in particular ansatz structure, we are able to find the optimal parameters minimizing the objective function. Normally, in the sense of operation, we can do the classical optimization process independently from other VQE parts, and even with your problem-specific concerns, and appears that you can develop your optimization algorithm for general variational issues.

*Constrained Optimization BY Linear Approximation (COBYLA).* One of the most powerful derivative-free methods, which has been favored by many users in lately decades, COBYLA makes use of linear interpolation of the objective function at each iteration by a unique linear polynomial function at the vertices for finding an optimal vector parameter within the trust region, then feeding the optimal point evaluated to the objective function to get the value improving the next iteration of approximation [38–41]. In VQE, COBYLA's linear interpolation at each step is a classical subroutine running on the CPU using only one objective value from the QPU evaluation running. And so, because of ignored derivative information, it would beneficially avoid several problems in analysis optimizations, especially Barren plateaus landscape, in return for less accuracy for more parameters ( $p > 9$ ) [41]. For a bird's-eye view, new updates to COBYLA versions

like UOBYQA, NEWUOA, and BOBYQA count the objective function's curvature information to increase convergence [42–44].

*Finite Difference (FD).* Let's dawn on one of the primary first-order derivative-based approaches, where the parameter  $\theta \in \mathbb{R}^p$  is updated at the  $k$ -th iteration by

$$\theta_{k+1} = \theta_k - \eta_k \nabla f(\theta_k), \quad (14)$$

which we usually name the Gradient Descent (GD) method. Finite Difference is a numerical technique to calculate the gradient vector  $\nabla f(\theta_k)$  without the analytical function's texture, which is the basic one used in the gradient descent method. We use the well-known central difference formula,

$$\nabla f(\theta_k)_i \simeq \frac{f(\theta_k + \epsilon \vec{i}) - f(\theta_k - \epsilon \vec{i})}{2\epsilon}, \quad (15)$$

where  $\vec{i} \in \mathbb{R}^p$  is  $i$ -th the unit vector and  $\epsilon$  is an infinitesimal change, with the error proportional to  $\mathcal{O}(\epsilon^2)$ . The smaller  $\epsilon$  we use, the more exact the result we get. However, due to the restricted accuracy of a classical computer, we are unable to achieve a value of  $\epsilon$  that is too small, which even becomes greater when implemented on a quantum device, where at least the sample error enters the picture.

*Simultaneous Perturbation Stochastic Approximation (SPSA).* To surmount some of the obstacles that arise from gradient descent operation on near-term devices, the idea of a perturbing stochastic approximation method is a good choice. SPSA generates an unbiased estimator  $\tilde{f}(\theta_k)$  of the gradient by simultaneously randomly perturbing the gradient direction of parameters [45], we replace the ordinary gradient vector  $\nabla f(\theta_k)$  by

$$\nabla f(\theta_k) \rightarrow \nabla \tilde{f}(\theta_k) = \frac{f(\theta_k + s_k \vec{\Delta}_k) - f(\theta_k - s_k \vec{\Delta}_k)}{2s_k} \vec{\Delta}_k, \quad (16)$$

where  $\vec{\Delta}_k$  is a random perturbed vector sampled from the zero-mean distribution, usually, the Bernoulli distribution is used. We can see that all parameters are simultaneously shifted by a random amount ( $\pm s_k$ ), our computation, therefore, only requires two objective function evaluations per iteration. Whereas standard gradient computation time is scaled along with the number of parameters, the SPSA optimizer is, however, independent, which saves a lot of time as we work on a higher parameter regime. Besides that, noise from quantum circuit executions computing the objective value can be regarded as a stochastic perturbation part absorbed into the SPSA procedure. These advantages promote SPSA and its other versions to be efficient techniques in the NISQ era.

## B. Quantum Operation

As opposed to the classical ones, the quantum operations require further quantum information extracted

from the structure of the problem, such as the trial wave function. This sort of property inevitably entails the details throughout the problem analysis, especially regarding Ansatz Construction.

*Parameter-shift rules (PSR).* Inspired by the classical shift rules in the exact derivative computation of some special functions, we are successfully able to figure out the analytical value of the objective function's derivatives using quantum devices. For any kind of quantum gate that has the form

$$\hat{G}(\theta) = e^{-i\theta \hat{G}} \quad (17)$$

generated by the Hermitian operator  $\hat{G}$ . Suppose that we have an expectation value of  $\hat{H}$ , which is our objective function  $f(\theta) = \langle \psi(\theta) | \hat{H} | \psi(\theta) \rangle$  parametrized by  $\theta$ . The ansatz wave function  $|\psi(\theta)\rangle = \hat{U}(\theta) |\psi\rangle_I$  is made up of  $\hat{U}(\theta) = \hat{A} \hat{G}(\theta) \hat{B}$ , with  $\hat{A}, \hat{B}$  are other arbitrary operators. As a result, the partial derivative of the  $f(\theta)$  with respect to  $\theta$  is thus obtained via the parameter-shift rules [46]

$$\partial_\theta f(\theta) = s \left[ f(\theta + \frac{\pi}{4s}) - f(\theta - \frac{\pi}{4s}) \right]. \quad (18)$$

The partial derivative  $\partial_\theta = \frac{\partial}{\partial \theta}$  implies we can generalize to a set of multiple parameters  $\{\theta_i\}$ . The evaluation of  $f(\theta \pm \frac{\pi}{4s})$  can be easily run on quantum computers, and then the exact amplitude of the vector gradient is derived. Within the aim of this paper, the given parametric ansatz is made out of Pauli rotations, and  $s = \frac{1}{2}$  is selected accordingly. The state-of-the-art formalism for more generic PQCs is also able to be derived [47, 48].

*Quantum Natural Gradient Descent (QNG).* How to improve the convergence? The global fixed learning rate  $\eta_k$  is apparently not a good choice, as one does not be good sensitive to the model information with respect to parameter changes. Initially, many attempts try to tune the learning rate  $\eta_k$ , such as learning rate schedulers that vary  $\eta_k$  after an iteration, latterly, adaptive methods that count previous iteration values or capture the curvature of the objective function using the diagonal approximation of the Hessian (HES), where each  $\eta_k$  is the inverse Hessian's diagonal element instead of being equally fixed. Those methods suggest that we can embed further information, rather than only the gradient vector, to make the optimal step size for our variational quantum algorithms. Similarly to the classical counterpart using the Fisher Information Matrix (FIM), Quantum Natural Gradient Descent invokes the quantum geometry of the wave function, which can help us get the optimal spot faster. Namely, we transform to the Riemann parameter space using the metric  $g \in \mathbb{R}^{p \times p}$  of projected Hilbert space  $\mathcal{PH}$  instead of the current Euclidean space  $g = \mathbb{1}_{p \times p}$ . The update Eq. (14) turns to

$$\theta_{k+1} = \theta_k - \eta_k g^+(\theta_k) \nabla f(\theta_k), \quad (19)$$

$g^+(\theta_k)$  means it is a pseudo-inverse local metric. Riemann parameter space metric  $g$  is generally defined

$$ds^2 = g_{ij} d\theta_i d\theta_j. \quad (20)$$

The Hilbert space  $\mathcal{H}$  of "bare" quantum states reduces to the  $\mathcal{PH} = \mathcal{H}/U(1)$  space as we ignore the local phase  $U(1)$  of quantum states [49], the quantum distance in  $\mathcal{PH}$  is then based on to calculate the Riemann metric  $g$

$$\begin{aligned} ds^2 &= 1 - |\langle \psi_\theta, \psi_{\theta+d\theta} \rangle|^2 \\ &= 1 - \left| 1 + \frac{1}{2} \langle \psi_\theta | \partial_i \partial_j \psi_\theta \rangle d\theta_i d\theta_j + \langle \psi_\theta | \partial_i \psi_\theta \rangle d\theta_i \right|^2 \\ &= \text{Re}[G_{ij}] d\theta_i d\theta_j. \end{aligned} \quad (21)$$

We expand up  $|\psi_{\theta+d\theta}\rangle = |\psi_\theta\rangle + |\partial_i \psi_\theta\rangle d\theta_i + \frac{1}{2} |\partial_i \partial_j \psi_\theta\rangle d\theta_i d\theta_j$  upto second order in  $d\theta$ , where  $\partial_i = \frac{\partial}{\partial \theta_i}$ . The Quantum Geometry tensor (QGT)  $G_{ij} \in \mathbb{R}^{p \times p}$  has two parts: the anti-symmetric imaginary part  $\sigma_{ij} = -\sigma_{ji}$  related to the gauge field of  $U(1)$  eventually vanishes, the only contribution comes from the real symmetric part  $g_{ij} \equiv g_{ij}(\theta)$  reflects the quantum distance in  $\mathcal{PH}$  space, where its formula is

$$g_{ij}(\theta) = \text{Re} [\langle \partial_i \psi_\theta | \partial_j \psi_\theta \rangle - \langle \partial_i \psi_\theta | \psi_\theta \rangle \langle \psi_\theta | \partial_j \psi_\theta \rangle]. \quad (22)$$

The Fubini-Study metric tensor  $g_{ij}(\theta)$  is a quantum analogue of the Fisher information matrix (QFIM). Given that it is proportional to  $p^2$ , the complicated computing and computational cost of  $g(\theta)$  is high and incompatible with the short-term quantum device. To solve this problem, an approximation strategy is required.

*Quantum Natural Gradient - Block Diagonal Approximation (QN-BDA).* Moreover, apart from Diagonal Approximation, where we just count  $p$  elements in the diagonal line, the QN-BDA employing the Parametric Family circuit is conveniently deployed entirely in the computation of the approximated metric tensor on the quantum computer [50]. The parametric unitary operator  $\hat{U}(\theta)$  acts on the initial state,  $|\psi\rangle_I$  entailing  $L$  layers

$$\hat{U}(\theta) = S_L P_L(\theta^L) \dots S_1 P_1(\theta^1), \quad (23)$$

where:

- $S_l$  are the static parts, which usually denote the entanglement layer.
- $P_l(\theta^l)$  are the parametric parts, which can be decomposed to single qubit gates  $P_l(\theta^l) = \bigotimes_{i=1}^N R_i(\theta_i^l)$ .
- The single qubit gate  $R_i(\theta_i^l) = \exp\{i\theta_i^l K_i\}$  is constructed from the Hermitian generator  $K_i$  with the parameter  $\theta_i^l \in \theta^l = \{\theta_1^l, \dots, \theta_N^l\}$ .

Such a type of parametrized circuit, whose nice properties we can prospect to yield a block diagonal form of QGT running completely on the quantum processor, each block corresponding to each layered vector parameter  $\theta^l \in \theta = \theta^1 \oplus \dots \oplus \theta^L$ . We denote

$$\hat{U}_n^m = S_m P_m(\theta^m) \dots S_n P_n(\theta^n), \quad (24)$$

then  $\hat{U}(\theta) \equiv \hat{U}_1^L = \hat{U}_{l+1}^L S_l P_l(\theta^l) \hat{U}_1^{l-1}$ . The partial derivative state can be written in the form

$$\begin{aligned} |\partial_i \psi_\theta\rangle &= \partial_i \hat{U}(\theta) |\psi\rangle_I = \hat{U}_{l+1}^L S_l \partial_i P_l(\theta^l) \hat{U}_1^{l-1} |\psi\rangle_I \\ &= \hat{U}_l^L (iK_i) |\psi_\theta^{(l-1)}\rangle. \end{aligned} \quad (25)$$

Note that  $[K_i, K_j] = 0$  in each layer, the unitarity of  $\hat{U}_n^m$  and the overlap of partial derivative states tell us the block matrix element

$$\begin{aligned} g_{ij}^{(l)}(\theta) &= \langle \psi_\theta^{(l-1)} | K_i K_j | \psi_\theta^{(l-1)} \rangle \\ &\quad - \langle \psi_\theta^{(l-1)} | K_i | \psi_\theta^{(l-1)} \rangle \langle \psi_\theta^{(l-1)} | K_j | \psi_\theta^{(l-1)} \rangle \end{aligned} \quad (26)$$

of the block-diagonal form of the Fubini-Study metric

$$g_{ij}(\theta) = \begin{pmatrix} \theta^1 & \theta^2 & \dots & \theta^L \\ g^{(1)} & 0 & \dots & 0 \\ 0 & g^{(2)} & \dots & 0 \\ \vdots & \vdots & \ddots & \vdots \\ 0 & 0 & \dots & g^{(L)} \end{pmatrix}.$$

QN-BDA approximation involves  $L$  quantum evaluations and works well on models with weak correlation.

*Quantum Natural-Simultaneous Perturbation Stochastic Approximation (QN-SPSA).* Inheriting the SPSA idea to calculate the gradient, it is capable to put up generating the Hessian matrix with fewer evaluations, the so-called 2-SPSA. Normally, the HES or FIM matrix consumes  $\mathcal{O}(p^2)$  quantum expectation. QN-BDA enables us to turn to relying on the number of layers  $\mathcal{O}(L)$ , saving us lots of computational resources. Even further, QN-SPSA just only executes four quantum runs to obtain the full second-order derivative matrix. Let's consider the Hessian of the Fubini-Study metric,

$$H_{ij}(\theta) \equiv g_{ij}(\theta) = -\frac{1}{2} \partial_i \partial_j |\langle \psi_\theta, \psi_{\tilde{\theta}} \rangle|^2 \Big|_{\tilde{\theta}=\theta}, \quad (27)$$

which is just the Hessian form of Eq. (22) so that we can deploy the 2-SPSA method to generate the QN-SPSA matrix [51, 52]. We can see the equivalence,

$$\begin{aligned} -\frac{1}{2} \partial_i \partial_j |\langle \psi_\theta, \psi_{\tilde{\theta}} \rangle|^2 \Big|_{\tilde{\theta}=\theta} &= -\partial_i \text{Re} \{ \langle \psi_\theta, \psi_{\tilde{\theta}} \rangle \langle \psi_{\tilde{\theta}}, \partial_j \psi_\theta \rangle \} \Big|_{\tilde{\theta}=\theta} \\ &= -\text{Re} \{ -\langle \partial_i \psi_\theta, \partial_j \psi_\theta \rangle + \langle \partial_i \psi_\theta, \psi_\theta \rangle \langle \psi_\theta, \partial_j \psi_\theta \rangle \}, \end{aligned} \quad (28)$$

which is exactly the same as Eq. (22). Applying the 2-SPSA approach to compute the second-order derivative of the function  $F(\theta, \tilde{\theta}) = -\frac{1}{2} |\langle \psi_\theta, \psi_{\tilde{\theta}} \rangle|^2$  instead of our loss function  $f(\theta)$  as being in Newton method. The core estimator in second-order SPSA is perturbed by two ran-

dom vectors  $\vec{\Delta}_k^1, \vec{\Delta}_k^2 \in \mathcal{U}^p\{-1, 1\}$  at step  $k$ -th

$$\begin{aligned} \Delta F = \frac{-1}{2} & \left[ F(\boldsymbol{\theta}_k + s_k \vec{\Delta}_k^1 + s_k \vec{\Delta}_k^2, \boldsymbol{\theta}_k) \right. \\ & - F(\boldsymbol{\theta}_k + s_k \vec{\Delta}_k^1, \boldsymbol{\theta}_k) + F(\boldsymbol{\theta}_k - s_k \vec{\Delta}_k^1, \boldsymbol{\theta}_k) \\ & \left. - F(\boldsymbol{\theta}_k - s_k \vec{\Delta}_k^1 + s_k \vec{\Delta}_k^2, \boldsymbol{\theta}_k) \right], \end{aligned} \quad (29)$$

which is composed of four terms, corresponding to four quantum expectations we run on the quantum processor. Then, the Fubini-Study metric Eq. (27) is replaced by the QN-SPSA metric at  $k$ -th iteration

$$g^k(\boldsymbol{\theta}) \rightarrow \bar{H}^k(\boldsymbol{\theta}) = \frac{\Delta F}{4s_k^2} \left( \vec{\Delta}_k^1 \vec{\Delta}_k^{2T} + \vec{\Delta}_k^2 \vec{\Delta}_k^{1T} \right), \quad (30)$$

where  $\bar{H}^k(\boldsymbol{\theta}) \in \mathbb{R}^{p \times p}$  and  $s_k$  is a small positive hyper-parameter able to be tuned. The metric is, however, still too highly stochastic, so some helpful techniques are invoked to resolve that hitch, say, counting information from previous updates to smooth the estimator

$$\tilde{H}^k = \frac{k}{k+1} \tilde{H}^{k-1} + \frac{1}{k+1} \bar{H}^k, \quad (31)$$

eventually, because the estimator is still ill-conditioned and unstable. To satisfy the positive semi-definite warranting the local convex analysis and invertibility condition of  $\tilde{H}^k$ , the following replacement is needed accordingly,

$$\tilde{H}^k \rightarrow \sqrt{\tilde{H}^k \tilde{H}^k} + \beta \mathbb{1}, \quad (32)$$

where the second term  $\beta \mathbb{1} \in \mathbb{R}^{p \times p}$  corresponds to the invertibility condition. The effect from the geometry metric is suppressed as the positive regulator gets a huge value  $\beta \gg 0$ , which indeed reduces to the standard gradient descent scenario and is more unstable. Therefore, that, in turn, causes a larger deviation in the average sample result when  $\beta \rightarrow 0$ . That makes a constant regulator  $\beta$ , which is thus a trade-off between Quantum Natural information and numerical instability. Another regularization approach, called “half-inversion”, generalizes the power of the second-order derivative matrix to  $n$  instead of the usual ones  $-1$  corresponding to standard natural gradient and  $0$  standing for original gradient, given by [53].

*Quantum Natural-Simultaneous Perturbation Stochastic Approximation with Parameter-Shift Rule (QN-SPSA+PSR)* is our extension for the QN-SPSA+SPSA method. Although QN-SPSA+SPSA has smaller complexity when compared with other methods, this stochastic method seems so randomized and makes it harder to converge and less stable when it comes to a bigger cost function landscape. Here, we propose the QN-SPSA+PSR algorithm, which is inherent in approximating the Fubini-Study metric properties in a way of saving computational cost. However, instead of using the SPSA method to approximate the gradient of the cost function,

we use the analytical method to calculate the gradient by PSR, which would compensate for the instability of the stochastic approximation in the Fubini-Study metric and drive itself in the gradient direction. This is expected for more stable and faster convergence compared to the former QN-SPSA+SPSA method.

## IV. RESULTS AND DISCUSSION

### A. Complexity estimation

Derivative-based method efficiency			
$\nabla f(\boldsymbol{\theta})$	PSR	FD	SPSA
Comp. cost	2p	2p	2
$g(\boldsymbol{\theta})$	QN-BDA	QN-SPSA	Const
Comp. cost	L	4	0

TABLE I: Comparison of derivative-based optimization methods in terms of computational cost. The table presents different optimization algorithms with their associated computational costs, respectively. The methods included are Parameter Shift Rule (PSR), Finite Differences (FD), and Simultaneous Perturbation Stochastic Approximation (SPSA), referring to gradient estimation techniques; Quantum Natural Gradient with Block-Diagonal Approximation (QN-BDA), Quantum Natural Gradient with SPSA (QN-SPSA), and a constant learning rate (Const) for adaptive learning rate methods; where p is the number of parameters and L is the number of PQC layers of the same rotation generator.

In summary of the derivatives-based optimization framework, we tell apart two subroutines: gradient calculation and  $g(\boldsymbol{\theta})$  matrix evaluation. For gradient calculation, we got three approaches: PSR offering exact gradients of quantum ansatz structure, FD-a classical numerical method that approximates gradients, and SPSA-a stochastic approximation technique requiring only two function evaluations per iteration. For the  $g(\boldsymbol{\theta})$  matrix calculation, we generally have four methods: Const—an identity matrix; QN-BDA approximates the Fubini-Study metric using the block diagonal structure; and QN-SPSA, which stochastically approximates the Fisher Information Matrix (FIM) with only four evaluations per iteration. A method is a combination of the gradient and  $g(\boldsymbol{\theta})$ , such as QN-BDA+PSR, which implies the application of the QN-BDA technique and PSR for the estimation of the gradient.

We provide a rough assessment of the optimization methods, grounded in theoretical judgment, where you are able to read off their information from Tab. I and Fig.

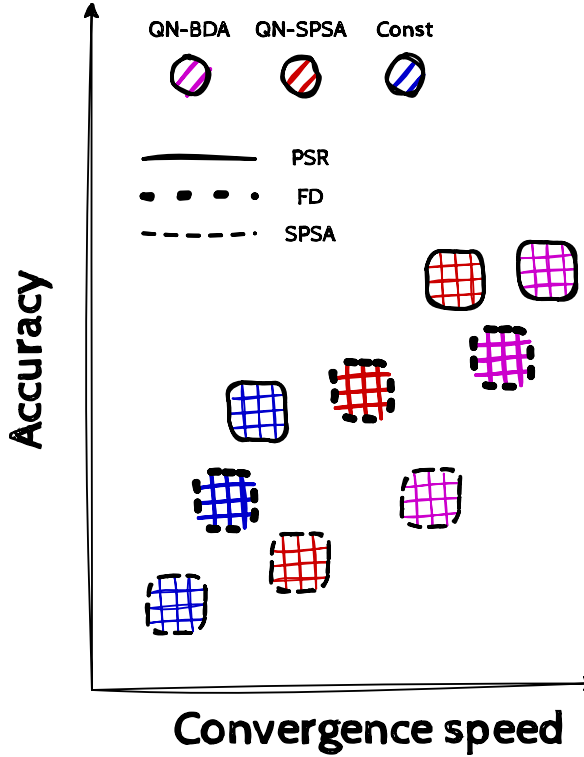


FIG. 3: The illustratively comparative graphics among combinations of gradient and adaptive learning rate methods in terms of accuracy and convergence speed.

The figure illustrates the performance of different optimization strategies, categorized by gradient estimation methods (PSR, FD, SPSA) and adaptive learning rate techniques (QN-BDA, QN-SPSA, Const). The results presented here are derived from the findings of previous works [45, 46, 50–52], alongside theoretical predictions and experimentally numerical scans conducted in this study.

3 for more illustrative purpose, demonstrating the trade-offs in performance and resource requirements among methods, e.g., computational cost, accuracy, and convergence speed. Tab. I is derived from the underlying theories of methods discussed above. Besides that, Fig. 3 provides an intuitive estimation based on theory-driven and bias-informed conjectures. In this estimation, the methods QN-BDA, QN-SPSA, and Const are ranked in descending order of convergence, accuracy, and computational cost. Similarly, for gradient methods, SPSA, FD, and PSR follow an ascending order of accuracy, convergence, and computational cost. Consequently, one can infer, for instance, that while the fully computed Hessian-like matrix+PSR should theoretically achieve the best performance at the expense of the intractably highest computational cost, the feasible approximate QN-BDA+PSR consumes much quantum overhead but is ex-

pected to outperform QN-SPSA+SPSA overall.

From this framework, a key motivation of the QN-SPSA+PSR algorithm is to merge the computational resource efficiency of QN-SPSA with the precision of the PSR. The computational cost of QN-SPSA, at four quantum evaluations per iteration, demonstrates remarkable scalability compared to traditional Hessian-based approaches like QN-BDA, which scale quadratically or linearly with the number of parameters and layers. While the PSR would keep the method at good stability and convergence. This refinement enables faster convergence and greater stability while maintaining a low computational overhead, highlighting its potential for practical application on NISQ devices. Notably, these are only theory-based rough estimations. In practice, the complexity of objective functions and the influence of noise would lead to variations in the performance of these methods, and approximate methods, such as methods using SPSA, would have advantages as noises come about. The experimentally numerical results, however, demonstrate an even better performance of QN-SPSA+PSR than predicted by the estimation, as we will present in the next section.

## B. Simulation results

We performed a detailed investigation of the VQE algorithm applied to the TIM model, testing several prominent optimization methods, ansatz structures, and entanglement configurations. Our simulations revealed several important insights into the performance of optimization methods and ansatz structures, highlighting the practical advantages of the proposed QN-SPSA+PSR algorithm. Remember that, if not specified, the external field and coupling constants were set to the default values  $h = 2$  and  $J = 1$ , respectively. For the stochastic methods, which are evaluated based on seven samples. The source code can be found at GitHub[54].

In Fig. 4, we use the RealAmplitudes ansatz, linear and full entanglement with 2 layers, to compare six different optimizations: SPSA, QN-BDA+PSR, FD, Cobyla, QN-SPSA+PSR, and QN-SPSA+SPSA. Noticeably, we observed that QN-SPSA+PSR outperforms Cobyla and Finite Difference methods. While the QN-BDA+PSR method did its job, as the theoretical prediction, showing the fastest convergence by direct use of the Fubini-Study metric tensor, QN-SPSA+PSR achieved comparable results with much lower computational overhead. By a small change in the gradient part from stochastic estimation to exact, we improved the performance of the inspired QN-SPSA+SPSA method, which made QN-SPSA+PSR more stable and faster convergence. Additionally, the classical derivative-free Cobyla exhibits a striking achievement, measuring up to QN-BDA+PSR and surpassing several algorithms while needing the least quantum overhead of cost function evaluation, one per iteration. That makes it a considerable method to im-

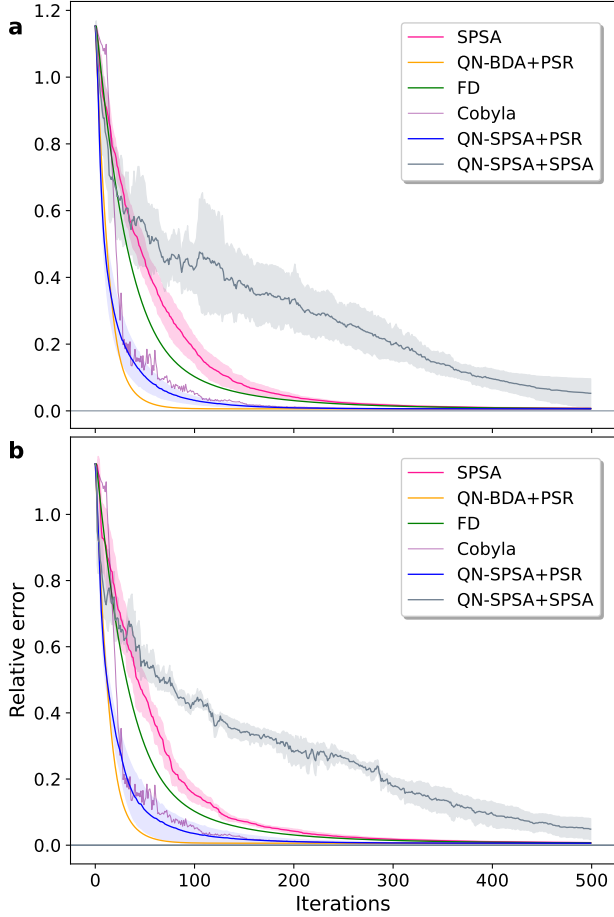


FIG. 4: Comparison of optimization methods for the TIM model with 12 spins using the RealAmplitudes ansatz. The plots show the relative error as a function of iterations for different optimization strategies applied to two entanglement mappings: (a) linear entanglement mapping and (b) full entanglement mapping. The plot illustrates the convergence behavior of each method, also showing the comparable results of the linear entanglement scheme to the full scheme, yet at a low quantum cost.

plement in the hybrid algorithm.

## V. CONCLUSION

The robustness of the QN-SPSA+PSR method further manifests using the more complex EfficientSU2 ansatz, which introduces a highly intricate cost function, shown in Fig. 5. Although EfficientSU2 ansatz would create a more complex cost function, QN-SPSA+PSR still shows stable and fast convergence properties and achieves results comparable to QN-BDA+PSR optimization. Whereas, QN-SPSA+SPSA and Cobyla showed signs of stagnation and requires more iterations to approach optimal solutions.

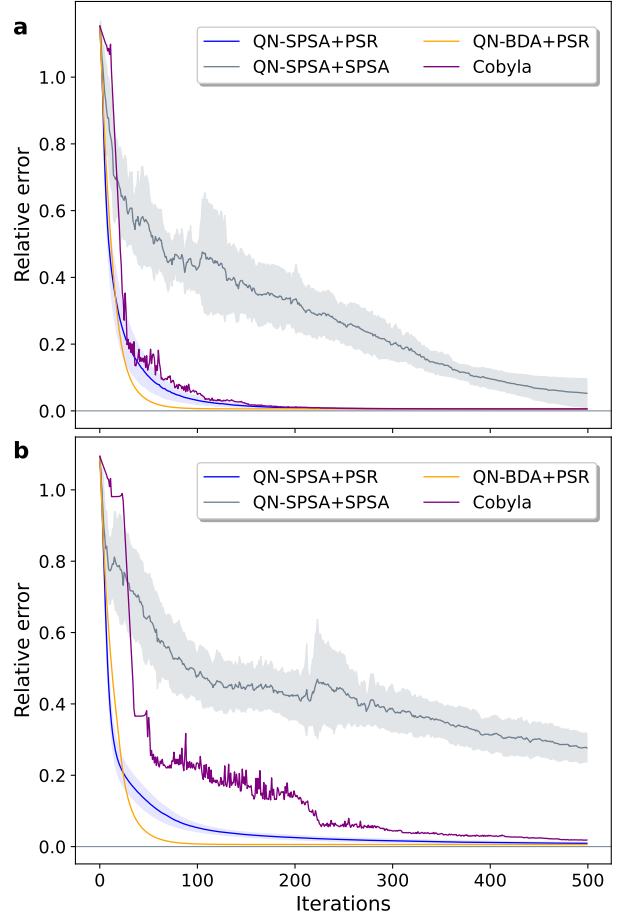


FIG. 5: Comparison of optimization methods for the TIM model with 12 spins using different ansatz configurations. The plots illustrate the relative error as a function of iterations for multiple optimization strategies applied to (a) the RealAmplitudes ansatz and (b) the EfficientSU2 ansatz. The visualized outcomes highlight the better and compatible performance of the RealAmplitudes ansatz for the TIM problem, as previously discussed in Section II C 2.

Furthermore, Figs. 4 and 5, which compared two types of ansatz and two types of entanglement schemes, turned out to show that linear entanglement is not much different than the full entanglement, and the RealAmp performed better in convergence than Efficient SU2. That proved the initial arguments aforementioned in Section II C 2, the RealAmplitude with linear entanglement, therefore, is good enough to survey the Ising model. Finally, the TIM energy estimates are obtained by varying external fields and numbers of spins, as illustrated in Figs. 6 and 7. In both cases, the QN-SPSA+PSR consistently delivered reliable and accurate results for the average ground state energy, closely aligning with the QN-BDA+PSR.

In this study, the research delved into the review of optimization algorithms, comparing quantum and classi-

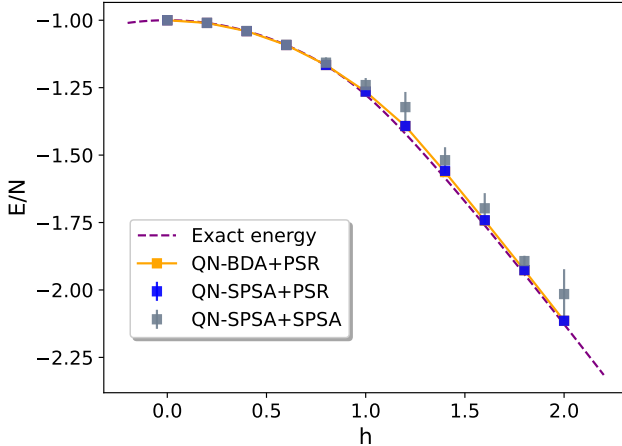


FIG. 6: Estimate the average ground state energy with QN-SPSA+SPSA, QN-SPSA+PSR, and QN-BDA+PSR for TIM of 12 spins and different external fields with the RealAmplitudes ansatz.

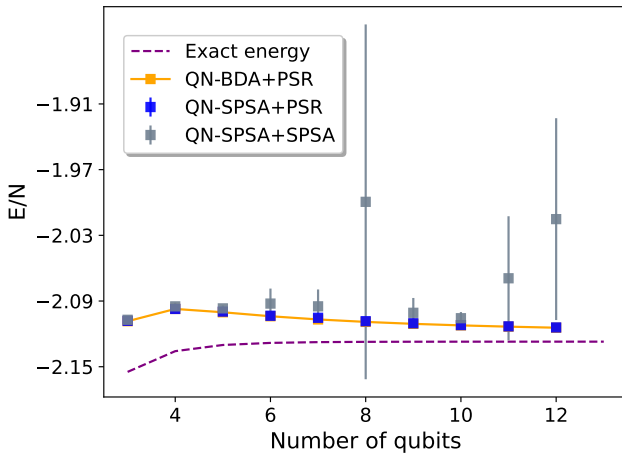


FIG. 7: Estimate the average ground state energy with QN-SPSA+SPSA, QN-SPSA+PSR, and QN-BDA+PSR for TIM of different numbers of spins with the RealAmplitudes ansatz.

cal algorithms to provide a bird's eye view. Moreover, leveraging the model's properties and symmetries, the analysis of the Ising Model was conducted to conjecture an ansatz form.

The results of the running indicated that the chosen

ansatz form, based on the Hamiltonian's properties, performed reasonably well, despite estimating the number of layers in Eq. 13 not necessarily being employed in this case. Nevertheless, it is believed to serve as a reasonably good initial estimation as the system scales up. Lastly, our exploration of optimization methods has yielded exciting outcomes. The newly proposed QN-SPSA+PSR algorithm exhibited unexpected results of computational efficiency, as it demonstrates potential not only in reducing computational overhead, as it does not scale up significantly with qubits like traditional Quantum Natural methods, but also in achieving more accurate optimal solutions. This work suggests promising prospects for further exploration and application of such an algorithm for future research endeavors in VQAs and NISQ devices.

## ACKNOWLEDGMENTS

The authors acknowledge helpful discussions and contributions from Triet Minh Ha. The numerical calculations in this work are performed using the high-performance computing systems at Phenikaa University. This work is financially supported by the Ministry of Education and Training of Vietnam under the grant number QG.20.17.

**Author contributions:** V.D. Nguyen and H.Q. Nguyen guided and supervised the project. The ideas and results were developed and carried out by D.T. Le and V.L. Nguyen, with support and discussions from V.D. Nguyen, H.Q. Nguyen, and H.C. Nguyen. D.T. Le wrote the manuscript with assistance from V.L. Nguyen and feedback from H.Q. Nguyen, V.D. Nguyen, and H.C. Nguyen. V.L. Nguyen packaged the code and executed the final summarization results on the HPC system.

**Data availability:** The datasets generated and analysed during the current study are available in the Variational-Quantum-Eigensolver repository, <https://github.com/nguyenvulinh666/Variational-Quantum-Eigensolver>.

## DECLARATIONS

**Competing interests:** The authors declare no competing interests.

[1] Marco Cerezo, Andrew Arrasmith, Ryan Babbush, Simon C Benjamin, Suguru Endo, Keisuke Fujii, Jarrod R McClean, Kosuke Mitarai, Xiao Yuan, Lukasz Cincio, et al. Variational quantum algorithms. *Nature Reviews Physics*, 3(9):625–644, 2021.

[2] Dave Wecker, Matthew B. Hastings, and Matthias Troyer. Progress towards practical quantum variational algorithms. *Phys. Rev. A*, 92:042303, Oct 2015.  
[3] John Preskill. Quantum computing in the nisq era and beyond. *Quantum*, 2:79, August 2018.

[4] Michael Brooks. Beyond quantum supremacy: the hunt for useful quantum computers. *Nature*, 574:19–21, 10 2019.

[5] Han-Sen Zhong, Hui Wang, Yu-Hao Deng, Ming-Cheng Chen, Li-Chao Peng, Yi-Han Luo, Jian Qin, Dian Wu, Xing Ding, Yi Hu, Peng Hu, Xiao-Yan Yang, Wei-Jun Zhang, Hao Li, Yuxuan Li, Xiao Jiang, Lin Gan, Guangwen Yang, Lixing You, Zhen Wang, Li Li, Nai-Le Liu, Chao-Yang Lu, and Jian-Wei Pan. Quantum computational advantage using photons. *Science*, 370(6523):1460–1463, December 2020.

[6] Frank Arute et al. Quantum supremacy using a programmable superconducting processor. *Nature*, 574(7779):505–510, 2019.

[7] Yulin Wu, Wan-Su Bao, Sirui Cao, Fusheng Chen, Ming-Cheng Chen, Xiawei Chen, Tung-Hsun Chung, Hui Deng, Yajie Du, Daojin Fan, Ming Gong, Cheng Guo, Chu Guo, Shaojun Guo, Lianchen Han, Linyin Hong, He-Liang Huang, Yong-Heng Huo, Liping Li, Na Li, Shaowei Li, Yuan Li, Futian Liang, Chun Lin, Jin Lin, Haoran Qian, Dan Qiao, Hao Rong, Hong Su, Lihua Sun, Liangyuan Wang, Shiyu Wang, Dachao Wu, Yu Xu, Kai Yan, Weifeng Yang, Yang Yang, Yangsen Ye, Jianghan Yin, Chong Ying, Jiale Yu, Chen Zha, Cha Zhang, Haibin Zhang, Kaili Zhang, Yiming Zhang, Han Zhao, Youwei Zhao, Liang Zhou, Qingling Zhu, Chao-Yang Lu, Cheng-Zhi Peng, Xiaobo Zhu, and Jian-Wei Pan. Strong quantum computational advantage using a superconducting quantum processor. *Physical Review Letters*, 127(18), October 2021.

[8] Frank Arute, Kunal Arya, Ryan Babbush, Dave Bacon, Joseph C Bardin, Rami Barends, Rupak Biswas, Sergio Boixo, Fernando GSL Brandao, David A Buell, et al. Quantum supremacy using a programmable superconducting processor. *Nature*, 574(7779):505–510, 2019.

[9] Kishor Bharti, Alba Cervera-Lierta, Thi Ha Kyaw, Tobias Haug, Sumner Alperin-Lea, Abhinav Anand, Matthias Degroote, Hermanni Heimonen, Jakob S Kottmann, Tim Menke, et al. Noisy intermediate-scale quantum (nisq) algorithms. *arXiv preprint arXiv:2101.08448*, 2021.

[10] Alberto Peruzzo, Jarrod McClean, Peter Shadbolt, Man-Hong Yung, Xiao-Qi Zhou, Peter J Love, Alán Aspuru-Guzik, and Jeremy L O’brien. A variational eigenvalue solver on a photonic quantum processor. *Nature communications*, 5(1):1–7, 2014.

[11] Edward Farhi, Jeffrey Goldstone, and Sam Gutmann. A quantum approximate optimization algorithm, 2014.

[12] Jarrod R McClean, Jonathan Romero, Ryan Babbush, and Alán Aspuru-Guzik. The theory of variational hybrid quantum-classical algorithms. *New Journal of Physics*, 18(2):023023, 2016.

[13] Jarrod R. McClean, Mollie E. Kimchi-Schwartz, Jonathan Carter, and Wibe A. de Jong. Hybrid quantum-classical hierarchy for mitigation of decoherence and determination of excited states. *Phys. Rev. A*, 95:042308, Apr 2017.

[14] D. J. ROWE. Equations-of-motion method and the extended shell model. *Rev. Mod. Phys.*, 40:153–166, Jan 1968.

[15] Oscar Higgott, Daochen Wang, and Stephen Brierley. Variational quantum computation of excited states. *Quantum*, 3:156, July 2019.

[16] Ken M. Nakanishi, Kosuke Mitarai, and Keisuke Fujii. Subspace-search variational quantum eigensolver for excited states. *Phys. Rev. Res.*, 1:033062, Oct 2019.

[17] M. Ganzhorn, D.J. Egger, P. Barkoutsos, P. Ollitrault, G. Salis, N. Moll, M. Roth, A. Fuhrer, P. Mueller, S. Woerner, I. Tavernelli, and S. Filipp. Gate-efficient simulation of molecular eigenstates on a quantum computer. *Phys. Rev. Appl.*, 11:044092, Apr 2019.

[18] César Feniou, Olivier Adjoua, Baptiste Claudon, Julien Zylberman, Emmanuel Giner, and Jean-Philip Piquemal. Sparse quantum state preparation for strongly correlated systems. *The Journal of Physical Chemistry Letters*, 15(11):3197–3205, 2024. PMID: 38483286.

[19] Changsu Cao, Jiaqi Hu, Wengang Zhang, Xusheng Xu, Dechin Chen, Fan Yu, Jun Li, Han-Shi Hu, Dingshun Lv, and Man-Hong Yung. Progress toward larger molecular simulation on a quantum computer: Simulating a system with up to 28 qubits accelerated by point-group symmetry. *Physical Review A*, 105(6), June 2022.

[20] P. J. J. O’Malley, R. Babbush, I. D. Kivlichan, J. Romero, J. R. McClean, R. Barends, J. Kelly, P. Roushan, A. Tranter, N. Ding, B. Campbell, Y. Chen, Z. Chen, B. Chiaro, A. Dunsworth, A. G. Fowler, E. Jeffrey, E. Lucero, A. Megrant, J. Y. Mutus, M. Neeley, C. Neill, C. Quintana, D. Sank, A. Vainsencher, J. Wenner, T. C. White, P. V. Coveney, P. J. Love, H. Neven, A. Aspuru-Guzik, and J. M. Martinis. Scalable quantum simulation of molecular energies. *Phys. Rev. X*, 6:031007, Jul 2016.

[21] J. I. Colless, V. V. Ramasesh, D. Dahmen, M. S. Blok, M. E. Kimchi-Schwartz, J. R. McClean, J. Carter, W. A. de Jong, and I. Siddiqi. Computation of molecular spectra on a quantum processor with an error-resilient algorithm. *Phys. Rev. X*, 8:011021, Feb 2018.

[22] Abhinav Kandala, Antonio Mezzacapo, Kristan Temme, Maika Takita, Markus Brink, Jerry M. Chow, and Jay M. Gambetta. Hardware-efficient variational quantum eigensolver for small molecules and quantum magnets. *Nature*, 549(7671):242–246, sep 2017.

[23] Isaac L. Chuang Michael A. Nielsen. *Quantum Computation and Quantum Information: 10th Anniversary Edition*. Cambridge University Press, New York, 2010.

[24] Y. Cao, J. Romero, and A. Aspuru-Guzik. Potential of quantum computing for drug discovery. *IBM Journal of Research and Development*, 62(6):6:1–6:20, 2018.

[25] Nick S. Blunt, Joan Camps, Ophelia Crawford, Róbert Izsák, Sebastian Leontica, Arjun Mirani, Alexandra E. Moylett, Sam A. Scivier, Christoph Sünderhauf, Patrick Schopf, Jacob M. Taylor, and Nicole Holzmann. Perspective on the current state-of-the-art of quantum computing for drug discovery applications. *Journal of Chemical Theory and Computation*, 18(12):7001–7023, November 2022.

[26] Vincenzo Lordi and John Nichol. Advances and opportunities in materials science for scalable quantum computing. *MRS Bulletin*, 46, 07 2021.

[27] Yudong Cao, Jonathan Romero, Jonathan P. Olson, Matthias Degroote, Peter D. Johnson, Mária Kieferová, Ian D. Kivlichan, Tim Menke, Borja Peropadre, Nicolas P. D. Sawaya, Sukin Sim, Libor Veis, and Alán Aspuru-Guzik. Quantum chemistry in the age of quantum computing. *Chemical Reviews*, 119(19):10856–10915, August 2019.

[28] Bela Bauer, Sergey Bravyi, Mario Motta, and Garnet Kin-Lic Chan. Quantum algorithms for quantum chemistry and quantum materials science. *Chemical Reviews*, 120(22):12685–12717, October 2020.

[29] Sergio Boixo, Sergei V. Isakov, Vadim N. Smelyanskiy, Ryan Babbush, Nan Ding, Zhang Jiang, Michael J. Bremner, John M. Martinis, and Hartmut Neven. Characterizing quantum supremacy in near-term devices. *Nature Physics*, 14(6):595–600, April 2018.

[30] Alexander J. McCaskey, Zachary P. Parks, Jacek Jakowski, Shirley V. Moore, T. Morris, Travis S. Humble, and Raphael C. Pooser. Quantum chemistry as a benchmark for near-term quantum computers, 2019.

[31] Jules Tilly, Hongxiang Chen, Shuxiang Cao, Dario Picozzi, Kanav Setia, Ying Li, Edward Grant, Leonard Woessnig, Ivan Rungger, George H Booth, et al. The variational quantum eigensolver: a review of methods and best practices. *arXiv preprint arXiv:2111.05176*, 2021.

[32] Dmitry A. Fedorov, Bo Peng, Niranjan Govind, and Yuri Alexeev. Vqe method: A short survey and recent developments, 2021.

[33] Edward Grant, Marcello Benedetti, Shuxiang Cao, Andrew Hallam, Joshua Lockhart, Vid Stojanovic, Andrew G. Green, and Simone Severini. Hierarchical quantum classifiers. *npj Quantum Information*, 4(1), dec 2018.

[34] Giuseppe Carleo and Matthias Troyer. Solving the quantum many-body problem with artificial neural networks. *Science*, 355(6325):602–606, 2017.

[35] Xavier Bonet-Monroig, Ryan Babbush, and Thomas E. O’Brien. Nearly optimal measurement scheduling for partial tomography of quantum states. *Phys. Rev. X*, 10:031064, Sep 2020.

[36] Daochen Wang, Oscar Higgott, and Stephen Brierley. Accelerated variational quantum eigensolver. *Physical Review Letters*, 122(14), apr 2019.

[37] P.G. de Gennes. Collective motions of hydrogen bonds. *Solid State Communications*, 1(6):132–137, 1963.

[38] M. J. D. Powell. Direct search algorithms for optimization calculations. *Acta Numerica*, 7:287–336, 1998.

[39] Michael JD Powell. A view of algorithms for optimization without derivatives. *Mathematics Today-Bulletin of the Institute of Mathematics and its Applications*, 43(5):170–174, 2007.

[40] Andrew R Conn, Katya Scheinberg, and Ph L Toint. On the convergence of derivative-free methods for unconstrained optimization. *Approximation theory and optimization: tributes to MJD Powell*, pages 83–108, 1997.

[41] Michael JD Powell. A direct search optimization method that models the objective and constraint functions by linear interpolation. In *Advances in optimization and numerical analysis*, pages 51–67. Springer, 1994.

[42] Michael JD Powell. Uobyqa: unconstrained optimization by quadratic approximation. *Mathematical Programming*, 92(3):555–582, 2002.

[43] Michael JD Powell. The newuoa software for unconstrained optimization without derivatives. In *Large-scale nonlinear optimization*, pages 255–297. Springer, 2006.

[44] Michael JD Powell. The bobyqa algorithm for bound constrained optimization without derivatives. *Cambridge NA Report NA2009/06, University of Cambridge, Cambridge*, 26, 2009.

[45] James C Spall. An overview of the simultaneous perturbation method for efficient optimization. *Johns Hopkins apl technical digest*, 19(4):482–492, 1998.

[46] Maria Schuld, Ville Bergholm, Christian Gogolin, Josh Izaac, and Nathan Killoran. Evaluating analytic gradients on quantum hardware. *Physical Review A*, 99(3), mar 2019.

[47] Leonardo Banchi and Gavin E. Crooks. Measuring Analytic Gradients of General Quantum Evolution with the Stochastic Parameter Shift Rule. *Quantum*, 5:386, January 2021.

[48] David Wierichs, Josh Izaac, Cody Wang, and Cedric Yen-Yu Lin. General parameter-shift rules for quantum gradients. *Quantum*, 6:677, March 2022.

[49] Ran Cheng. Quantum geometric tensor (fubini-study metric) in simple quantum system: A pedagogical introduction, 2010.

[50] James Stokes, Josh Izaac, Nathan Killoran, and Giuseppe Carleo. Quantum natural gradient. *Quantum*, 4:269, may 2020.

[51] Julien Gacon, Christa Zoufal, Giuseppe Carleo, and Stefan Woerner. Simultaneous perturbation stochastic approximation of the quantum fisher information. *Quantum*, 5:567, oct 2021.

[52] Andrea Mari, Thomas R. Bromley, and Nathan Killoran. Estimating the gradient and higher-order derivatives on quantum hardware. *Phys. Rev. A*, 103:012405, Jan 2021.

[53] Tobias Haug and M. S. Kim. Optimal training of variational quantum algorithms without barren plateaus, 2021.

[54] The code in this work can be accessed at the electronic address: <https://github.com/nguyenvulinh666/Variational-Quantum-EigenSolver>.